British Journal of Applied Science & Technology
17(5): 1-9, 2016, Article no.BJAST.29023
ISSN: 2231-0843, NLM ID: 101664541

SCIENCEDOMAIN *international*
www.sciencedomain.org

Influence of Pole Numbers to Field Weakening Characteristics of Interior Permanent Magnet Motor for Electric Vehicle Application

Pudji Irasari[1], Muhammad Kasim[1*], Muhammad Fathul Hikmawan[1], Puji Widiyanto[1] and Ketut Wirtayasa[1]

[1]Research Centre for Electrical Power and Mechatronics, Indonesian Institute of Sciences, Indonesia Komplek LIPI, Jl. Sangkuriang, Gd.20, Bandung 40135, Indonesia.

Authors' contributions

This work was carried out in collaboration between all authors. Authors PI and MK designed, analyzed as well as managed literature researches. Authors PW and KW performed literature research and author MFH managed the technical drawing of the design. All authors read and approved the final manuscript.

Article Information

DOI: 10.9734/BJAST/2016/29023
Editor(s):
(1) Rodolfo Dufo Lopez, Electrical Engineering Department, University of Zaragoza, Spain.
Reviewers:
(1) Rajinder Tiwari, Amity University, India.
(2) Hermes José Loschi, States University the Campinas, Brazil.
(3) Jian-Long Kuo, National Kaohsiung First University of Science and Technology, Taiwan.
Complete Peer review History: http://www.sciencedomain.org/review-history/16386

Original Research Article

Received 18th August 2016
Accepted 15th September 2016
Published 29th September 2016

ABSTRACT

High torque and wide field weakening region are two parameters needed for electric vehicle. In order to achieve those requirements, variation of pole numbers of an interior permanent motor utilizing the same stator geometry is performed in this study. Slot harmonics are also compared in connection with the losses produced. All calculation are analytically performed and the motor characteristic is presented in the form of torque versus speed graph.

Keywords: Pole numbers; interior permanent magnet motor; slot harmonics; torque; field weakening region.

**Corresponding author: E-mail: kasime99uh@yahoo.co.id;*

1. INTRODUCTION

Until recently, permanent magnet synchronous machines (PMSMs) are considered as the most capable of competing with induction machines for electric vehicles applications. One of the contributing factors is the ease in obtaining magnet with high energy product, such as NdFeB, with reasonable price. In addition, employing PMSMs have also some advantages including less noise, compact volume, high efficiency, high power density, fast dynamics and high torque to inertia ratio [1,2].

Among diverse types of PMSMs, interior permanent magnet (IPM) motor is the most preferably for its superiorities, specifically low torque ripple and acoustic noise, and topology in terms of stator layout and rotor arrangement that can be varied [3]. Optimized designs of IPM have been approached through various methods, for instance by improving the air gap flux density quality [4] or reducing the ripple torque [5,6].

In electric vehicle application, an electric machine is desired to have a wide speed range or a wide field weakening operation. Regarding this issue, two types of basic operation of PM brushless (PM BL) drives to improve field weakening operation are generally employed, namely PM BLAC and PM BLDC. PM BLAC drives operate with sinusoidal current and sinusoidal airgap flux so that they need a high-resolution position signal for closed-loop control, such as encoder or resolver, which is very costly. This type of drives can readily provide constant-power operation by using flux-weakening control. Meanwhile, PM BLDC drives operate with a rectangular current and a trapezoidal airgap flux so that they just require a low-cost discrete position sensor for phase-current commutation, such as Hall devices. For the PM BLDC drives, constant-power operation is more complex as flux-weakening control needs d-q-coordinate transformation, which is unsuitable for the rectangular-fed PM BLDC motors. However, a control scheme, namely, advanced conduction angle control, can significantly extend the constant power operating range of PM BLDC motor drives [7-9].

The configuration of permanent magnet on the rotor also affects field weakening characteristic. In [10], surface permanent magnet (SPM) and IPM motor drives for EV application are compared. At a given inverter and active part size, the continuous power generated by both SPM and IPM motors is comparable. Nevertheless the IPM motor has a very good overload capability over the entire speed range, while the output power of the SPM motor cannot overcome the continuous power rating independently of the applied current overload.

Another method of improving field weakening region is discussed in [11]. In this study, 45 kW Tooth-Coil PMSM with different slot-pole combinations, 12/10 and 18/16, were investigated. These machines have high synchronous winding factors, balanced radial magnetic pulls and relatively low leakage factors. Low number of poles allows operation at relatively low supply frequencies which decreases the losses in the whole drive. Hence, high efficiency and high torque can be achieved with these slot- and pole-combinations together with a wide constant power speed range.

Unfortunately, compared to other type of motor, PMSMs have the least speed range region [1,12] and for that reason, researchers keep introducing new mechanisms to improve it. Reference [13] implementing torque control strategy both in lower speed and power constant regions as well as showing the crucial design parameters. New rotor structures of PMSM to enlarge field weakening region were proposed by [14,15].

It is already known that electric machines can also be a harmonic source since winding distributed in the stator slots never generates an ideal sinusoidal waveform. This results in distortion of magneto motive force [16]. Several common ways to reduce harmonics are performed by skewing either stator or rotor slots or permanent magnet, employing parallel branches, using fractional pitch, etc [3,17-19].

This study is aimed to obtain the best performance of IPM motor, in terms of the generated torque and field weakening region, by varying the pole numbers including 2, 4, 6 and 8 poles. Slot harmonics are calculated analytically and the motor is designed under the same stator dimension.

2. WINDING TYPE AND MOTOR INPUT PARAMETERS

The motor topology is illustrated in Fig. 1. The Curved magnet is applied to reduce cogging torque for uniform range to the stator teeth. Distance from the magnet surface to the rotor periphery is set at 1 mm. The pole configurations of all studied motors and the detailed dimensions

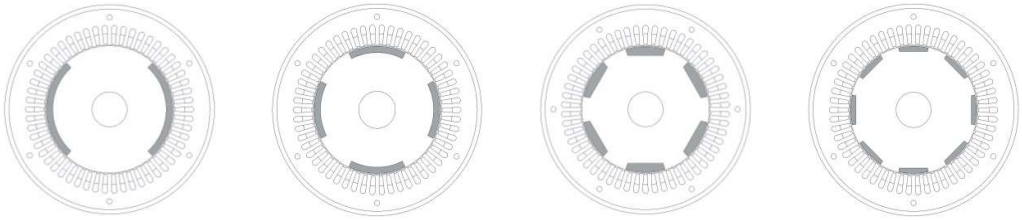

(a) (b) (c) (d)

Fig. 1. Motor pole configurations, (a) 2 poles, (b) 4 poles, (c) 6 poles, (d) 8 poles

of the given stator are presented in Fig. 1 above and Table 1 respectively.

The winding type is full-pitch concentric and the variation of the pole numbers are 2, 4, 6, 8, yielding either fractional or integer number of slots per pole per phase q, presented by:

$$q = \frac{S_{ss}}{2p \cdot m} \quad (1)$$

where q = number of slots per pole per phase, S_{ss} = number of stator slots, $2p$ = number of poles and m = number of phases. Number of phase winding at fundamental harmonic is:

$$N_{ph} = \frac{E_{ph}}{4.44 \cdot f \cdot \phi \cdot k_w} \quad (2)$$

with E_{ph} = back electromotive force (V), f = frequency (Hz), ϕ = magnetic flux (Wb), k_w = winding factor, B_g = air gap flux density (T), A_m = permanent magnet area (m^2), k_d = distribution factor, k_p = pitch factor, and k_s = skew factor.

Motor employs full pitch winding with terminal voltage of 220 V and current density of 5 A/mm^2. Detil dimension of the stator is presented in Fig. 2 and Table 1.

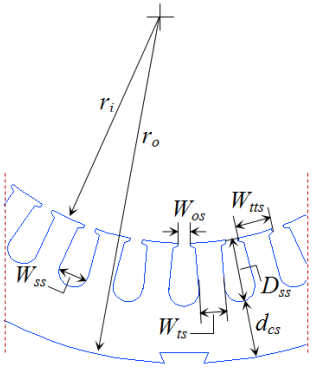

Fig. 2. Stator dimension [20]

3. HARMONICS OF WINDING FACTOR

The values of q on each studied motor either integer or fraction, always produce q > 1. Furthermore, the harmonics of the winding factor is calculated using conventional method according to [21], commenced by restating Equation (1) as:

$$q = \frac{S_{ss}}{2p \cdot m} = \frac{z}{n} \quad (3)$$

where z is the numerator of q and n is the denominator of q reduced to the lowest terms.

Table 1. Description of stator dimension

Description	Magnitude	Unit
Number of stator slots, Ss	54	
Number of slots per pole per phase	1	
Pitch factor	1	
Inner radius of stator, r_i	0.0738	m
Inner diameter of stator, D_i	0.1476	m
Outer radius of rotor, r_o	0.170	m
Outer diameter of rotor, D_o	0.340	m
Effective length of stator core, L_i	0.103	m
Height of stator yoke, d_{cs}	0.0412	m
Slot opening width, W_{os}	0.00288	m
Top tooth width, W_{tts}	0.00571	m
Tooth width, W_{ts}	0.0045	m
Slot width, W_{ss}	0.0112	m
Slot height, D_{ss}	0.0226	m
Stator slot area, A_{ss}	111.93	mm^2

In this study, the winding is two layers so that the harmonics can be created by the 1st-grade or the 2nd-grade, depends on the value of n. If n is even, the harmonics are for the 2nd-grade and vice versa. Following are the equations to obtain the harmonic orders:

for odd v/p,

$$\frac{v}{p} = \pm\frac{1}{n}(2mg + 1) \quad g = 0, \pm1, \pm2, \pm3, \ldots \quad (4)$$

and for even v/p,

$$\frac{v}{p} = \pm\frac{1}{n}(2mg + 2) \quad g = 0, \pm1, \pm2, \pm3, \ldots \quad (5)$$

The ± sign is chosen so that the equations have the positive sign for the fundamental (v = +1). Accordingly, the harmonics of the winding factor for q > 1 are:

for odd v/p,

$$k_w = \pm\frac{\sin\left[\frac{v}{p}\frac{\pi}{2m}\right]}{nq\sin\left[\frac{v}{p}\frac{\pi}{2nmq}\right]}\sin\left[\frac{v}{p}\frac{y}{mq}\frac{\pi}{2}\right] \quad (6)$$

for even v/p,

$$k_w = \pm\frac{\cos\left[\frac{v}{p}\frac{\pi}{2m}\right]}{nq\cos\left[\frac{v}{p}\frac{\pi}{2nmq}\right]}\sin\left[\frac{v}{p}\frac{y}{mq}\frac{\pi}{2}\right] \quad (7)$$

4. FIELD WEAKENING CHARACTERISTIC

In electric vehicle, motor performance is measured by its ability to attain wide speed range or wide field weakening region, which is highly influenced by the motor type and its control strategy as shown in Fig. 3.

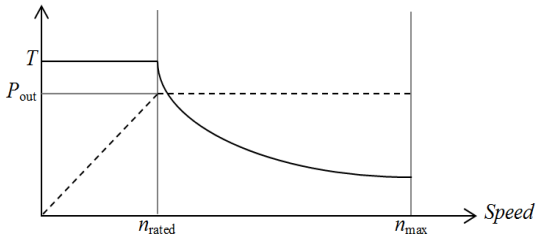

Fig. 3. Desired field-weakening drive characteristics in EV

Below the rated speed n_{rated}, electric motor drive produces high magnetic field to provide constant rated torque up to its rated speed or its rated power limit. This state is usually used for starting, climbing and accelerating whereas above the rated speed, the magnetic field is reduced, which is used for cruising [22,23]. In order to obtain a wider speed range, low flux linkage and high d-axis inductance is suggested [24].

The d- and q- axis inductances for IPM is given by:

$$L_d = \frac{6}{\pi}(q \cdot N_s \cdot k_w)^2 \ \frac{\mu_o}{\delta_e + \frac{l_m}{\mu_r}} r_i L_i \quad (8)$$

$$L_q = \frac{6}{\pi}(q \cdot N_s \cdot k_w)^2 \ \frac{\mu_o}{\delta_e} r_i L_i \quad (9)$$

where N_s = number of conductors per slot, μ_o = permeability of free space = $4\pi10^{-7}$, μ_o = relative permeability of the magnet = 1.1, δ_e = effective air gap including slot effect, l_m = magnet thickness.

The optimal design of IPM is fulfilled when

$$\psi_m = L_d \cdot I_n \quad (10)$$

where ψ_m = flux linkage and I_n = rated current.

Under this condition, the widest field weakening performance is achieved. Furthermore, the electromagnetic torque is [25],

$$T_e = \frac{mp}{\omega_r}\left[E_q I_q + \left(X_d - X_q\right) I_d I_q\right] \quad (11)$$

where γ = current angle, X_d, X_q = d- and q- axis reactances that can be calculated with,

$$X_d = \omega \cdot L_d; \qquad X_q = \omega \cdot L_q \quad (12)$$

and

$$E_q = E_a \quad (13)$$

The d-axis and q-axis components of current as well as the current angle are given by the following equations,

$$I_d = -I_{ph} \cdot sin\gamma \quad (14)$$

$$I_q = I_{ph} \cdot cos\gamma \quad (15)$$

$$\gamma = sin^{-1}\left[\frac{k_x^2 \cdot e_m^2 + k_x^2 \cdot \left(L/e_m\right)^2 - 1}{2 \cdot k_x^2 \cdot L}\right] \quad (16)$$

where e_m = the per-unit open circuit voltage at the corner point of the motor characteristic graph (Fig. 3), with the maximum r.m.s. a.c. voltage of the converter as the base voltage,

$$e_m = \frac{E_a}{V_t} \quad (17)$$

and

$$k = \frac{1}{e_m \cdot \sqrt{1-e_m^2}} = \frac{n_{max}}{n_{rated}} \quad (18)$$

$$L = e_m \cdot \sqrt{1 - e_m^2} \quad (19)$$

The maximum value of k_x is k.

5. RESULTS AND DISCUSSION

5.1 Harmonics of Winding Factor

Different number of poles yields different values of *q*, i.e. 9, $4\frac{1}{2}$, 3, $2\frac{1}{4}$, consecutively for 2, 4, 6 and 8 poles. Graphs of harmonic content of each pole are exhibited in Fig. 4.

It can be seen that for all values of *q*, the 3rd harmonic is eliminated as the motor is 3-phase star connection. Slot harmonics comes up in pair due to ± sign of *g*. With *q* = integer, the 2- and 6-pole motors have a symmetrical MMF so that only odd harmonics occur. In electric motor, harmonics distortion raises losses (copper loss and iron loss), which leads to excessive heating. Therefore, a sufficient cooling system should be provided. Losses of every studied motor is presented in the following section.

5.2 Motor Parameters and Characteristics

In the design, FF was set as a reference at the maximum value of 0.41 to obtain a comparable calculation of phase winding of all studied motor configuration. With respect to that matter, a trial and error simulation was performed to select wire diameter by applying one at a time the available commercial wire size so that FF was as close as possible to the set maximum value. This value was based on the manufacturing experience of the authors. Furthermore, motor parameters, such as winding number, resistance, inductance and etc. are presented in Table 2.

Core loss is highly affected by frequency and stator core volume. In this case, all motors have the same stator core volume so that core losses are changed proportionally only by the frequency. The most dominant loss is copper loss generated by three times of square of rated current flowing into conductor having a certain value of resistance. Copper loss gives big impact to the motor efficiency. In general, the studied motors express high efficiency, which is above 80%. Highlighting the motors with the efficiency of around 95%, it is one of the benefits of using permanent magnet machines. For comparison, such high efficiency of PMMs were studied by [3,26].

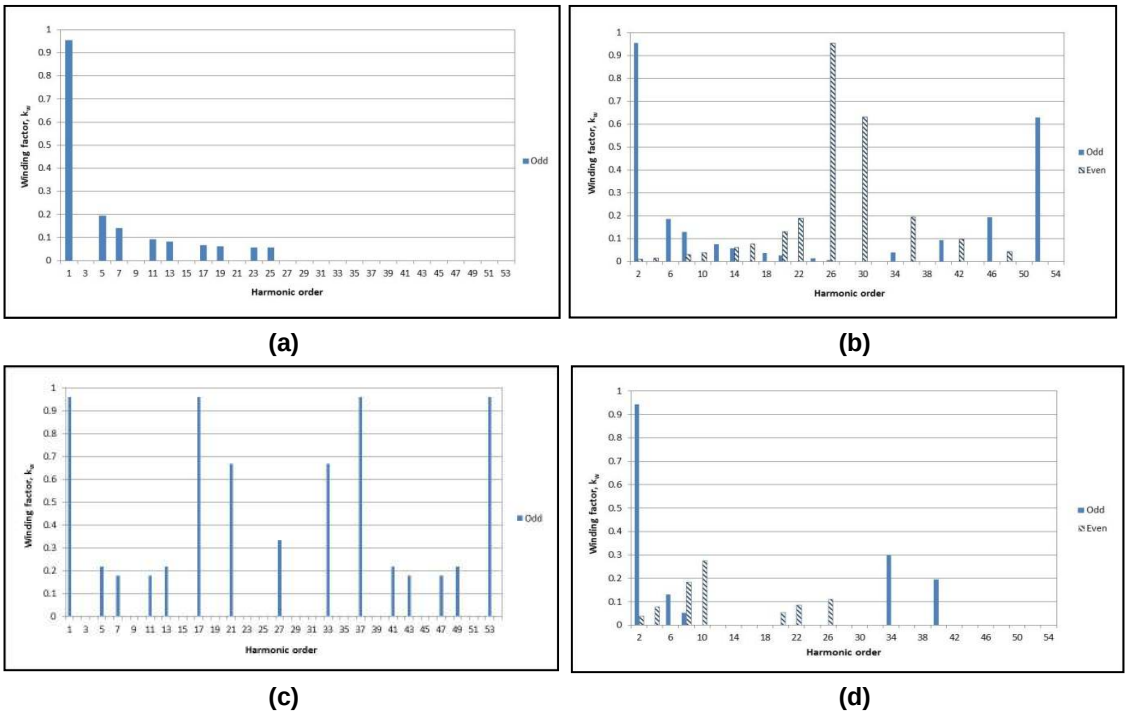

Fig. 4. Slot harmonic, (a) 2 poles, (b) 4 poles, (c) 6 poles, (d) 8 poles

Table 2. Calculation results of the motor parameters

Parameters	Magnitude					
Pole numbers	**2**			**4**		
Frequency, Hz	50	75	100	50	75	100
Phase winding numbers	162	108	82	154	88	76
Wire diameter, mm	1.8	2.3	2.5	1.8	2.0	2.5
FF	0.39	0.41	0.39	0.41	0.40	0.39
Resistance, Ω	0.96	0.40	0.25	0.67	0.22	0.17
L_d, mH	89.9	37.6	25.2	25.7	7.9	6.4
L_q, mH	160.3	67.1	44.9	45.8	14.1	11.4
ψ_m, weber	1.1435	0.7809	0.6179	0.3269	0.3189	0.1570
n_{rated}, rpm	3000	4500	6000	1500	2250	3000
n_{max}, rpm	15000	22500	30000	3701	4245	5108
n_{max}/n_{rated}	5	5	5	2.47	1.89	1.70
Rated current, A	12.72	20.77	24.54	12.72	22.62	24.54
Rated power, kW	2.30	4.00	4.87	5.23	9.54	10.38
Rated torque, Nm	20.75	22.63	20.84	48.13	58.32	48.31
Copper loss, W	465.8	514.8	447.4	325.2	331.3	313.3
Core loss, W	13.3	26.3	43.5	13.3	26.3	43.5
Efficiency, %	82.3	81.9	90.3	94.9	95.9	92.6

Table 2. Calculation results of the motor parameters (continue)

Parameters	Magnitude					
Pole numbers	**6**			**8**		
Frequency, Hz	50	75	100	50	75	100
Phase winding numbers	210	144	108	308	202	150
Wire diameter, mm	1.5	1.9	2	1.2	1.5	1.8
FF	0.38	0.41	0.41	0.37	0.38	0.41
Resistance, Ω	1.1	0.46	0.26	2.78	1.16	0.60
L_d, mH	12.4	5.5	3.1	27.3	6.25	6.4
L_q, mH	23.2	10.3	5.8	48.6	20.5	11.5
ψ_m, weber	0.1096	0.0780	0.0487	0.1542	0.0553	0.0127
n_{rated}, rpm	1000	1500	2000	750	1125	1500
n_{max}, rpm	1700	2693	3432	1802	2317	2935
n_{max}/n_{rated}	1.70	1.80	1.72	2.40	2.06	2.0
Rated current, A	8.84	14.18	19.01	5.65	8.84	12.72
Rated power, kW	5.54	9.00	12.15	4.67	7.43	10.80
Rated torque, Nm	51.10	55.30	56.04	42.00	44.89	48.91
Copper loss, W	251.4	275.1	276.6	266.4	272.0	292.4
Core loss, W	13.3	26.3	43.5	13.3	26.3	43.5
Efficiency, %	94.9	96.2	96.9	93.8	95.6	96.4

From the equation above, it can be seen that the field weakening characteristic is affected by many parameters. Noticing motor with the same number of poles, the constant power region (n_{max}/n_{rated}) is wider at lower frequency for 4 and 8 poles but for 2- and 6-poles motors, it can be said that the increase in frequency does not affect their field weakening characteristics. Regular pattern is shown by L_d and ψ_m where their values go down/is drop/ fall with the increase of frequency. Regarding the torque, in general, the motors show the highest value at 75 Hz.

The field weakening characteristic of every motor in Table 2 is presented in the form of torque vs. speed graph as shown in Fig. 5. The best field

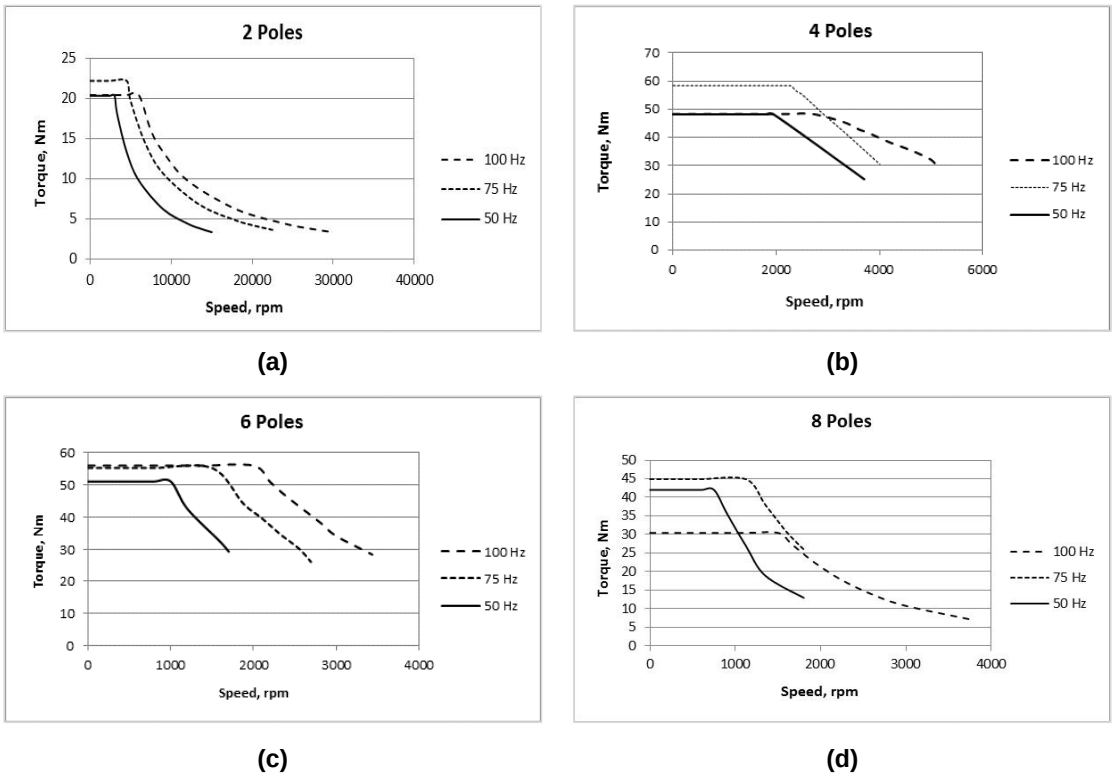

Fig. 5. Field weakening characteristic, (a) 2 poles, (b) 4 poles, (c) 6 poles, (d) 8 poles

weakening characteristic is shown by 2-poles motor which indicates the widest constant power region, which is up to 5 times of the base speed, but they suffer from low rated torque. An ideal motor drive performance is required to have both wide field weakening region and high rated power or torque.

Observing the maximum speeds of the 4-, 6-, and 8-pole motors, they are well below that of the 2-pole motors. Nevertheless, for some cases, maximum speed of around 3000 – 3500 rpm [12] or twice of n_{rated} is acceptable as motor is usually connected with a drivetrain in a vehicle system. Accordingly, the 4-pole motors are the most potential candidates, especially the one with 50 Hz of rated torque or having the highest n_{max}/n_{rated}.

Looking more closely at (Figs. 5b-d), it can be seen that torque constant and power constant regions are almost balance. According to [23] this kind of characteristic is suitable for industrial application. However, there is still possibilities to enlarge power constant or field weakening region by implementing certain methods as mentioned earlier. This should be optimally done due to an inverse relationship between torque and speed. As for rated torque, it appears an irregular enhancement with the increase of number of poles from 2 to 8. only 4- to 8-pole motors that can produce torque around 50 Nm attained at different frequencies. The highest torque is demonstrated by 75 Hz of 6-pole motor.

6. CONCLUSION

Effect of pole numbers to field weakening characteristic of interior permanent magnet motor has been discussed in this paper. Slot harmonics are also analyzed in relation with the losses produced. Simulation results indicate that the best field weakening characteristic is obtained when the poles are 2-poles followed by poor maximum torque. In contrast, the 4-, 6- and 8-pole motors demonstrate high maximum torque yet bad field weakening region. Having almost 2.5 of the maximum speed to the rated speed ratio, the 4-pole motor with 50 Hz of frequency presents the best performance for electric vehicle application. Regarding the 6-, and 8-pole motors, future work to improving their field weakening regions is still needed.

COMPETING INTERESTS

Authors have declared that no competing interests exist.

REFERENCES

1. Isfahani AH, Sadeghi S. Design of a permanent magnet synchronous machine for the hybrid electric vehicle. International Journal of Electrical, Computer, and Systems Engineering. 2008;2:1-5.
2. Liu CS, Hwang JC, Cheng CP. Design of permanent magnet synchronous motor with low cogging torque. In: The 2010 International Power Electronics Conference. 2010;1083-1087.
3. Chen HS, Dorrell DG, Tsai MC. Design and operation of interior permanent-magnet motors with two axial segments and high rotor saliency. IEEE Trans Magn. 2010;46:3664-3675.
4. Zhao Ch, Li Si, Yan Yg. Influence factor analysis of pmsmair gap flux density. In: Proceedings of the Eighth International Conference on Electrical Machines and Systems; Nanjing, China; 27-29 September. 2005;334-339.
5. Lim S, Min S, Hong JP. Low torque ripple rotor design of the interior permanent magnet motor using the multi-phase level-set and phase-field concept. IEEE Trans Magn. 2012;48:907-910.
6. Lim S, Min S, Hong JP. Level-set-based optimal stator design of interior permanent-magnet motor for torque ripple reduction using phase-field model. IEEE Trans Magn. 2011;47:3020-3023.
7. Jinyun G, Chau KT, Chan CC, Jiang JZ. A new surface-inset, permanent-magnet, brushless DC motor drive for electric vehicles. IEEE Trans Magn. 2000;36: 3810-3818.
8. Liu Y, Zhu ZQ, Howe D. Direct torque control of brushless DC drives with reduced torque ripple. In: Industry Applications Conference - 39th IAS Annual Meeting. 2004;2390-2396.
9. Chau KT, Chan CC, Liu C. Overview of permanent-magnet brushless drives for electric and hybrid electric vehicles. IEEE Trans Ind Electron. 2008;55:2246-2257.
10. Vagati A, Pellegrino G, Guglielmi P. Comparison between SPM and IPM motor drives for EV application. In: XIX International Conference on Electrical Machines (ICEM). 2010;1-6.
11. Ponomarev P, Lindh P, Pyrhonen J. Effect of slot-and-pole combination on the leakage inductance and the performance of tooth-coil permanent-magnet synchronous machines. IEEE Trans Ind Electron. 2013;60:4310-4317.
12. Finken T, Hameyer K. Design of electric motors for hybrid- and electric-vehicle applications. In: 12th International Conference on Electrical Machines and Systems; Tokyo, Japan; 2009.
13. Meyer M, Bocker J. Optimum control for interior permanent magnet synchronous motors (ipmsm) in constant torque and flux weakening range. In: The 12th International Power Electronics and Motion Control Conference; Portoroz: August 30-September 1. 2006;282-286.
14. Stumberger B, Hamler A, Trlep M, Jesenik M. Analysis of interior permanent magnet synchronous motor designed for flux weakening operation. IEEE Trans Magn. 2001;37:3644-3647.
15. Baoquan K, Chunyan L, Shukang C. Flux-weakening-characteristic analysis of a new permanent-magnet synchronous motor used for electric vehicles. IEEE Trans Plasma Sci. 2011;39:511-515.
16. Birbir Y, Nogay HS. Voltage and current harmonic variations in three-phase induction motors with different stator coil pitches. International Journal of Energy. 2007;1:122-129.
17. Frauman P, Burakov A, Arkkio A. Effects of the slot harmonics on the unbalanced magnetic pull in an induction motor with an eccentric rotor. IEEE Trans Magn. 2007; 43:3441-3444.
18. Boldea I, Nasar SA, The Induction Machine Handbook. Florida: CRC Press; 2000.
19. Buksnaitis J. Methods for determination of winding factors of alternating-current electric machines. Elektron Elektrotech. 2009;89:83-86.
20. Irasari P. Metode perancangan generator magnet permanen berbasis pada dimensi stator yang sudah ada. Ketenagalistrikan dan Energi Baru Terbarukan. 2008;7:15-27.
21. Salminen P. Fractional slot permanent magnet synchronous motors for low speed applications. PhD Thesis, Lappeenranta University of Technology Lappeenranta, Finland; 2004.
22. Schneider T, Koch T, Binder A. Comparative analysis of limited field

weakening capability of surface mounted permanent magnet machines. IEE P-Elec Pow Appl. 2004;151:76-82.
23. Xue XD, Cheng KWE, Cheung NC. Selection of electric motor drives for electric vehicles. In: Australian Universities Power Engineering Conference; Sydney, NSW, AUS: 14-17 Decemeber. 2008;1-6.
24. Chin YK, Soulard J. A theoretical study on premanent magnet synchronous motor for electric vehicle. In: Sixth International Power Engineering Conference; Singapore: NTU; 27-29 November. 2003; 435-440.
25. Miller TJE. Brushless permanent-magnet and reluctance motor drives. New York: Oxford University Press; 1993.
26. Lindh P, Nerg J, Pyrhonen J, Polikarpova M, Jussila H, Rilla M. Interior permanent magnet motors with non-overlapping concentrated windings or with integral slot windings for traction application. Prz Elektrotechniczn. 2012;88: 9-12.

Peer-review history:
The peer review history for this paper can be accessed here:
http://sciencedomain.org/review-history/16386